



Tetraethylorthosilicate-assisted interfacial polymerization for the fabrication of polyamide thin-film nanocomposite reverse osmosis membranes with enhanced desalination performance

Yulin Wei¹, Han Zhang¹, Guiru Zhu*, Zhaofeng Liu, Guojia Ji, Congjie Gao

College of Chemistry and Chemical Engineering, Ocean University of China, Qingdao 266100, China, Tel. +86-0532-66782552; emails: zhugr@ouc.edu.cn (G. Zhu), zhuimengyichang@126.com (Y. Wei); 837001493@qq.com (H. Zhang); liuzhaofeng126@126.com (Z. Liu); 285898697@qq.com (G. Ji); gaocjie@ouc.edu.cn (C. Gao)

Received 2 April 2018; Accepted 28 December 2018

ABSTRACT

The high-performance polyamide reverse osmosis nanocomposite membrane for desalination was prepared by tetraethylorthosilicate (TEOS)-assisted interfacial polymerization (IP) of 1,3-phenylenediamine in the aqueous phase with 1,3,5-benzenetricarbonyl trichloride in the organic phase on polysulfone ultrafiltration supports. The different contents of TEOS and different IP time were investigated. TEOS is slightly soluble in water and partially hydrolyzed under alkaline conditions. The addition of TEOS during the IP process not only influenced the IP as a co-solvent but also generated inorganic nanoparticles in the polyamide layer in situ as nanofillers to form thin-film nanocomposite membrane. The permeability test showed that the polyamide nanocomposite membrane prepared with 20 wt.% TEOS possesses improved desalination performance. The water flux increased more than twice the pure polyamide composite membrane, and the rejection has been maintained over 95%.

Keywords: TEOS; Interfacial polymerization; RO nanocomposite membrane; Desalination; In situ

1. Introduction

With the rapid development of the global economy, the problem of water shortage has become increasingly prominent. Seawater or brackish water desalination is one of the important ways to solve the serious shortage of water resources. In recent years, desalination technology based on reverse osmosis (RO) membrane has attracted extensive attention because of its environment-friendly and low energy consumption [1–4]. However, the current cost of producing fresh water by RO technology is still high, which limits its widespread use in desalination. At present, polyamide thin-film composite (TFC) membrane prepared by interfacial

polymerization (IP) method is widely used in RO technology [5,6]. In order to improve the separation performance (especially increase the water flux) of the polyamide TFC membrane, researchers have studied a variety of methods to optimize the polyamide membrane. The large quantity and high quality of freshwater from desalination depends on high water flux and high salt rejection, respectively. Therefore, the effective membrane-modified methods should avoid the trade-off between flux and rejection.

Among the modification methods, the addition of additives (solid and liquid) in organic phase or aqueous phase during the polymerization process has attracted wide attention because the preparation process is same as that

¹ Co-first authors

* Corresponding author.

of the pure polyamide composite membrane without additional steps. In 2007, Jeong et al. [7] reported the formation of zeolite-polyamide thin-film nanocomposite (TFN) RO membrane by dispersing zeolite into the organic phase during the IP, which lead to RO membrane with dramatically improved water permeability. Since then, many nanoparticles and nanotubes have been used as the nanofillers to prepare the TFN membrane, and the enhanced separation performance has been obtained [8–15]. Kong et al. [16,17] reported an IP procedure by adding acetone into the organic phase, which was referred to as co-solvent-assisted interfacial polymerization (CAIP). Polyamide membranes prepared via CAIP possess controlled thin dense layer and effective nanopores, which results in high water flux and no considerable salt rejection loss. Since then, different types of organic solvents such as ethyl acetate, diethyl ether, toluene, isopropyl alcohol, and *N,N'*-dimethyl formamide have been used as co-solvent in the CAIP method to improve the permeate property of the TFC membrane [18,19]. The results showed that water flux and salt rejection could be controlled by the types and amount of co-solvents added into organic phase. Although the addition of additives, both solid nanomaterials and liquid organic compound, can effectively improve the separation performance of the polyamide composite membrane, there are still inherent shortcomings.

It is found that the uniform dispersion of solid nanomaterial in the organic or aqueous phase is difficult due to the incompatibility between inorganic nanoparticles and solvent, when the nanomaterial was used as nanofiller to prepare TFN membrane. Furthermore, when higher amount of nanomaterials were added, the agglomeration would occur and lead to the deflection of the membrane. On the other hand, liquid additives can be easily dispersed in the organic phase, which overcomes the shortcoming of the addition of inorganic nanomaterials. However, the organic compound would remove out during IP, heat treatment, and immersion in DI water, making the membrane with loose structure. Our previous study shows that the loose structure of the membrane prepared by CAIP method will be compacted under higher operation pressure, leading to the decline of water flux [20].

The metal alkoxide can solute in organic solvent and can transform to nanoparticles by hydrolysis and condensation reaction. Therefore, it is possible to generate nanoparticles in situ into/on the polymer matrix of membrane. The composite membranes containing silica nanoparticles formed in situ by dispersing the tetraethylorthosilicate (TEOS) in casting solution were reported [21–27]. These studies reported composite membranes fabricated by the phase-inversion process to form polyvinylidene fluoride, polyvinyl alcohol (PVA), polyethersulfone, polyvinyl chloride, and polyether imide membranes and introduced inorganic nanoparticles into membranes successfully. Noteworthy, silane cross-linked PVA/chitosan (CS) membrane was prepared by CS/PVA/TEOS and was applied to the RO process [27]. Another kind of organosilane *bis*(triethoxy silyl)ethane was used to modify the ultrafiltration membrane and nanofiltration membrane via the surface coating method, and enhanced performance was obtained [28,29]. Kong et al. [30] reported the nanocomposite polyamide membrane prepared by metal-alkoxide-assisted IP. The nanocomposite membrane

prepared with phenyltriethoxysilane showed 2-fold water flux compared with the pure membrane with no rejection loss. It indicates that metal alkoxide can form nanoparticles in situ during the IP process.

However, to the best of our knowledge, the addition of TEOS in organic phase during the IP to form silica nanoparticles in situ has not been reported. Therefore, it is important to investigate the influence of the more common TEOS on the performance of polyamide composite membrane. The TEOS was added to the organic phase assisting the IP to fabricate the polyamide nanocomposite membrane. The influence of TEOS on the structure and performance of polyamide nanocomposite membrane was investigated by scanning electron microscopy (SEM), energy-dispersive spectroscopy (EDS), Fourier transform infrared (FT-IR), contact angle, and so on.

2. Experimental

2.1. Materials

Sodium dodecyl sulfate (SDS), 1,3,5-benzenetricarbonyl trichloride (TMC, 98%), and 1,3-phenylenediamine (MPD, >99%) were obtained from Aladdin Co. Ltd (China). TEOS (98%) and *n*-hexane were obtained from Sinopharm Chemical Reagent Co. Ltd (Shanghai, China). All chemicals were analytical grade and used without further purification. Ultrafiltration polysulfone (PSF) support was purchased from Hangzhou Water Treatment Center (China).

2.2. Membrane fabrication

The polyamide nanocomposite membranes were prepared by IP assisted with TEOS on the PSF support. The detailed process is as follows. First, the PSF support was placed in an aqueous solution of 2 wt.% MPD and 0.15 wt.% SDS for 2 min, and then the excess aqueous solution was removed. After drying, the soaked PSF support was immersed in a hexane solution of 0.1 wt.% TMC and 0–35 wt.% TEOS for 5 min. Then, the excess organic phase solution was removed, and the membrane was dried for 2 min at room temperature followed by heat treatment at 80°C for 5 min. Finally, the prepared membranes were immersed in deionized water to remove unreacted monomer and solvent.

2.3. Characterization

The surface morphology of the resultant membrane was investigated by SEM (HitachiS-4800, Japan). The samples were deposited on sample holders with adhesive carbon foil and were sputtered with gold before measurement. The hydrophilicity of the membrane was determined through the sessile drop method with a contact angle analyzer (KRüSSDSA100, Germany). An FT-IR spectrum was recorded by FT-IR spectrometer (Bruker TENSOR27, Germany).

2.4. RO performance

The RO performance was characterized by measuring the water flux and salt rejection through cross-flow permeation test on the RO performance evaluation equipment (Fig. 1) with an effective membrane area of 19.6 cm² and

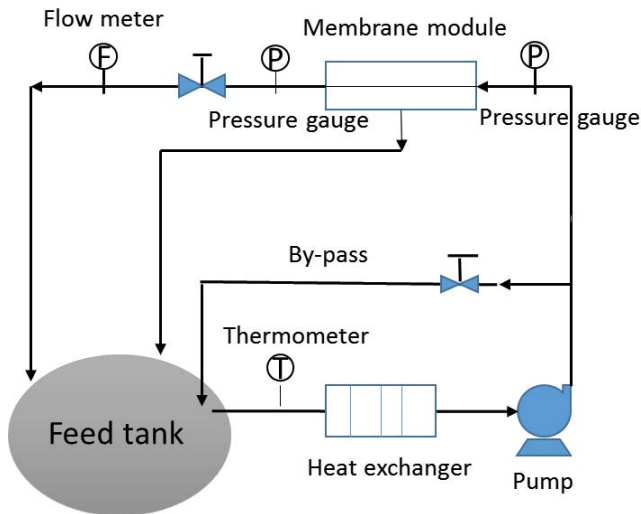


Fig. 1. Permeability test equipment schematic diagram.

operating pressure of 1.6 MPa at 25°C. An aqueous solution of 2,000 ppm NaCl was used as feed solution. The water flux was measured after pre-compressed for 0.5 h at 1.8 MPa.

Salt rejection (R , %) and water flux (F , $L\ m^{-2}h^{-1}$) were calculated with the following Eqs. (1) and (2), respectively:

$$R = \left(1 - \frac{C_2}{C_1}\right) \times 100\% \quad (1)$$

$$F = \frac{V}{S \times t} \quad (2)$$

where C_1 ($mg\ L^{-1}$) is the feed concentration, C_2 ($mg\ L^{-1}$) is the permeate concentration, V is the permeate volume (L), t is the permeate time (h), and S is the effective membrane area (m^2).

3. Results and discussion

3.1. Influence of IP time

The permeability properties of the pure polyamide composite membrane prepared by the conventional IP method and the nanocomposite membrane prepared by TEOS-assisted IP method are shown in Fig. 2. With the extension of the IP time, the water flux of the pure polyamide membrane decreased from 22.1 to 14.8 $L\ m^{-2}h^{-1}$ with all the salt rejection over 97%. It was believed that the longer IP time would lead to thicker polyamide layer, resulting in the decrease of water flux [31]. When the IP took for 1 min, the nanocomposite membrane prepared by adding 15 wt.% TEOS in organic phase had high water flux (88 $L\ m^{-2}h^{-1}$) and low salt rejection (30%). It indicated that the effective polyamide layer cannot form during 1 min of IP assisted with TEOS, although 1 min of IP time was usually chosen to prepare the pure polyamide membrane and the other nanocomposite membrane. When the IP time reached 3 min, the water flux decreased to 32.1 $L\ m^{-2}h^{-1}$ and the salt rejection increased to 94.5%. Further prolonging the IP time to 5 min,

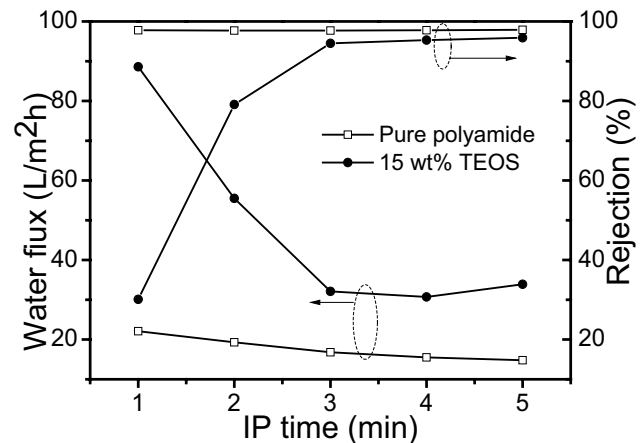


Fig. 2. Permeability properties of the pure polyamide composite membrane and the nanocomposite membrane prepared by adding 15 wt.% TEOS in organic phase as a function of time of interfacial polymerization (IP).

the water flux remains unchanged with the salt rejection increased to 95.9%, similar to the pure polyamide membrane. It showed that the TEOS may influence the IP process. In order to balance the water flux and the rejection and considering the slow hydrolysis of TEOS, the nanocomposite membranes prepared by TEOS-assisted IP were fabricated via IP for 5 min.

3.2. Characterization of the membranes

3.2.1. Scanning electron microscopy

Fig. 3 shows the surface morphologies of pure polyamide membranes with different IP times (a , b) and the nanocomposite membranes prepared with different TEOS contents (c – g). The surface morphology of the pure polyamide membrane prepared with IP time for 1 min clearly shows the typical ridge-and-valley structure (Fig. 3(a)), which is the common morphology of polyamide layer with large roughness and surface area [32]. The surface morphology of the pure polyamide membrane prepared with IP time for 5 min exhibits larger leaf-like structure (Fig. 3(b)). The change of the surface morphology was due to the thicker polyamide layer with longer IP time. It was the reason that the water flux decrease with the longer IP time (Fig. 2).

The less widespread polyamide layer can be clearly detected on the surface of the membrane prepared with less amount of TEOS (0.5 wt.%) (Fig. 3(c)), although the ridge-and-valley structure of the modified membrane is similar to the pure polyamide layer (Fig. 3(b)). The ridge-and-valley structure of the modified membrane changed to widespread layer with the increased content of TEOS (Fig. 3(d)–(g)). The widespread polyamide layer structure was similar to the membranes prepared assisted by organic compound as co-solvents. It indicated that the TEOS could work as co-solvent during the IP process. It is believed that the co-solvent added in the organic phase was intended to form a narrow miscibility zone, which led to the thicker reaction zone, resulting in widespread polyamide layer structure [17].

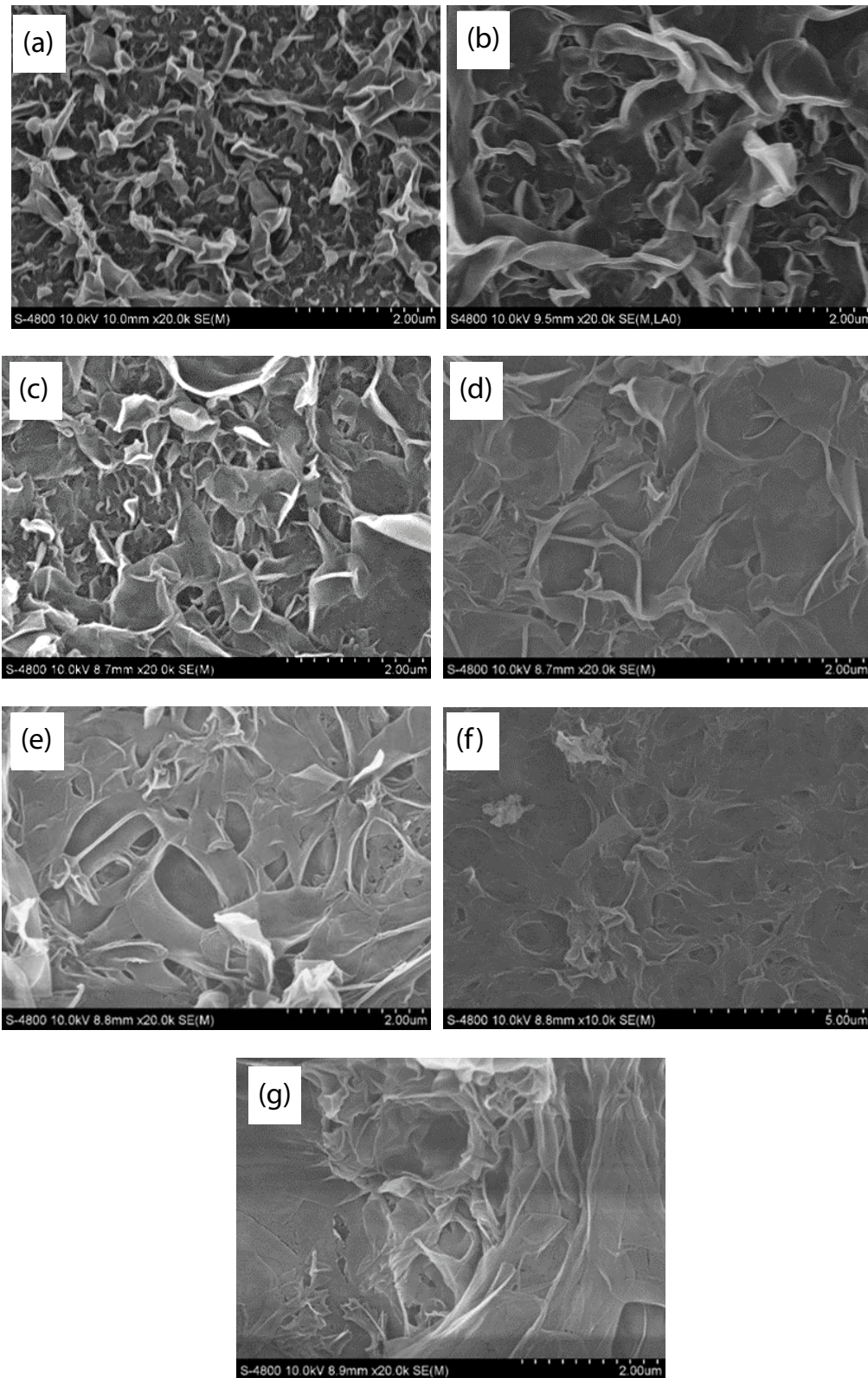


Fig. 3. SEM surface images of the pure polyamide membranes prepared with different IP time: (a) 1 min and (b) 5 min, and the nanocomposite membranes prepared by adding different TEOS contents with IP time for 5 min: (c) 0.5 wt.%, (d) 5 wt.%, (e) 10 wt.%, (f) 20 wt.%, and (g) 35 wt.%.

3.2.2. Energy-dispersive spectroscopy

The Si peak can be detected in the EDS spectrum in Fig. 4(b), which is absent from the pure polyamide membranes in Fig. 4(a). The Si element was from the TEOS, indicating that the TEOS resided in the polyamide layer during the IP process, heat treatment, and immersion in DI water. TEOS is a kind of metal alkoxide, which can hydrolyze and condense to form solid particles. The nanocomposite membranes were calcined at 550°C in order to remove the polymer materials in the membrane. After calcining, white powder was obtained, and the EDS of the white powder was shown in Fig. 4(c). The Si peak with high intensity is found in Fig. 4(c), indicating the white powder consisting mainly of oxides and silicon.

3.2.3. Fourier transform infrared

Fig. 5 shows FT-IR spectra of the pure polyamide membrane, the nanocomposite membrane prepared with 35 wt.% TEOS, and silica nanoparticles. All polyamide membranes showed the typical spectra of polyamides which were polymerized by MPD and TMC [17]. The vibrational band at about 1,660 cm^{-1} (amide I) was assigned to C=O stretch, the band around 1,540 cm^{-1} (amide II) was belonging to C–N stretch, and the band around 1,609 cm^{-1} was due to polyamide aromatic ring breathing [17]. The bands at about 1,090 and 800 cm^{-1} were evidently identified in the spectra of the nanocomposite membrane prepared with 35 wt.% TEOS, which was similar to the polyamide membranes incorporated with hydrophilic SiO_2 nanoparticles [33]. The antisymmetric stretching vibrational band of Si–O–Si was around 1,090 cm^{-1} and the symmetrical stretching vibrational band of Si–O was near 800 cm^{-1} . This character confirms that the TEOS was converted to SiO_2 in the polyamide membrane.

3.2.4. Contact angle

Water contact angle is an important parameter to reflect the membrane surface hydrophilicity. In general, the smaller

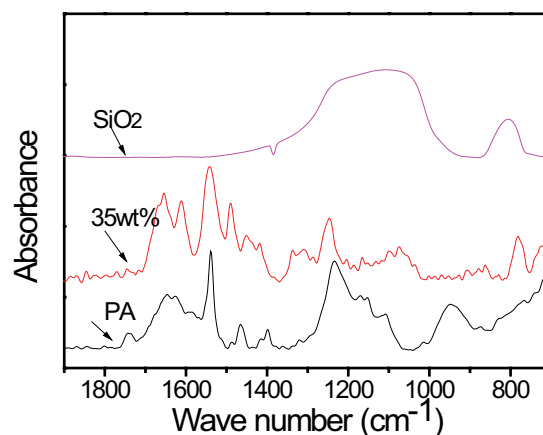


Fig. 5. FT-IR spectra of the pure polyamide membrane (PA), the nanocomposite membrane prepared with 35 wt.% TEOS, and silica nanoparticles (SiO_2).

the contact angle value, the more hydrophilic the membrane [34]. Fig. 6 shows that the contact angle decreases with the addition of TEOS, indicating the increase of hydrophilicity of the membrane with TEOS. There were some carboxyl groups (by hydrolysis of the unreacted acid chloride) and amino groups on the surface of the polyamide layer, which resulted in a certain hydrophilicity of the membrane. It was believed that the degree of cross-linking of polyamide layer would be decreased with the addition of co-solvent [16]. And, the low cross-linking of the polyamide layer with the addition of TEOS into the organic phase could introduce more carboxyl and amino groups in the polyamide layer. This was the reason for the increase in the hydrophilicity of the membrane prepared assisted with TEOS. Some co-solvents such as alcohols, esters, and ketones did not change or react during the IP process and heat treatment and could be eliminated during the formation of polyamide layer. Different from the above compounds, TEOS would undergo hydrolysis and

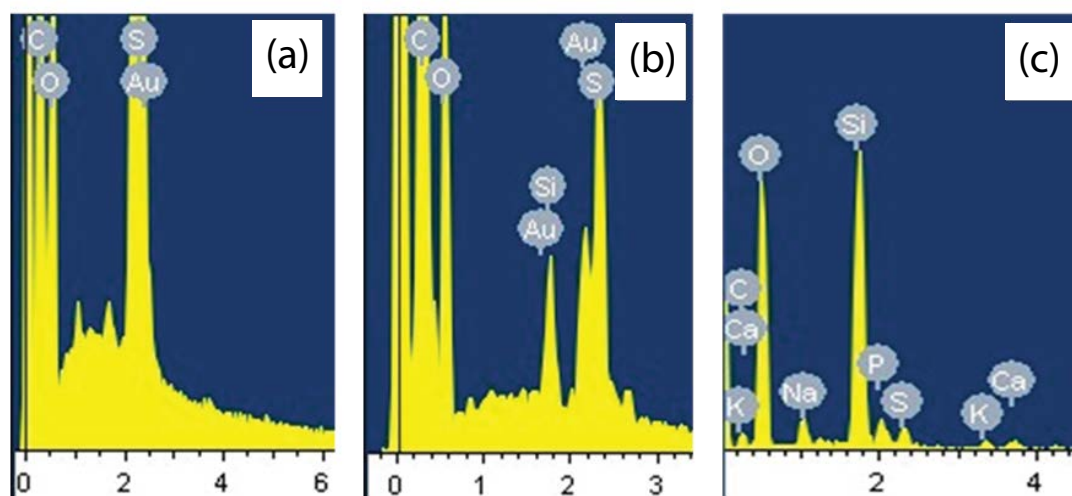


Fig. 4. EDS of (a) pure polyamide composite membrane, (b) the nanocomposite membrane prepared with 20 wt.% TEOS, and (c) calcination residue of the nanocomposite membrane prepared with 20 wt.% TEOS.

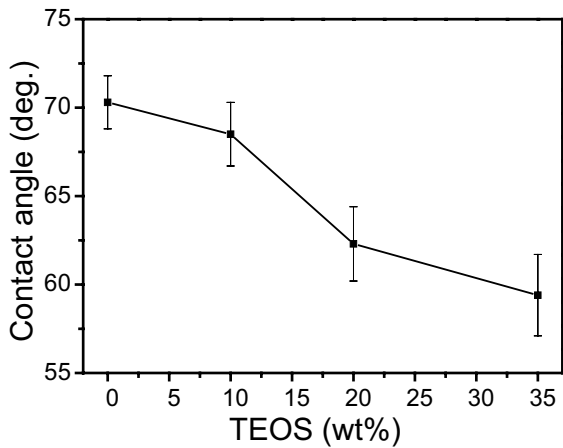


Fig. 6. Contact angles of the nanocomposite membranes prepared with different TEOS contents.

condensation, resulting in solid silica particles. Moreover, the solid silica particles had hydroxyl groups on the surface, which contributed the increase of hydrophilicity of the modified membrane.

3.2.5. RO performance

Fig. 7 shows the salt rejection and water flux trends of the nanocomposite membranes prepared with different TEOS contents. With the increase of TEOS content from 0 wt.% to 20 wt.%, the water flux of the membrane obviously increased from 14.8 to 37.6 L m⁻²h⁻¹ and the salt rejection slightly decreased from 97.9% to 95.5%. The TEOS could act as a co-solvent during the IP process, resulting in the polyamide layer with lower cross-linking degree. The lower cross-linking degree made the polyamide layer with higher hydrophilicity and larger pore, which contributed to the increase of water flux and decrease of salt rejection. However, when the addition of TEOS reached 35 wt.%, the salt rejection sharply reduced to 75%, although the water flux increased to 45.6 L m⁻²h⁻¹. It indicated that the excessive amount of

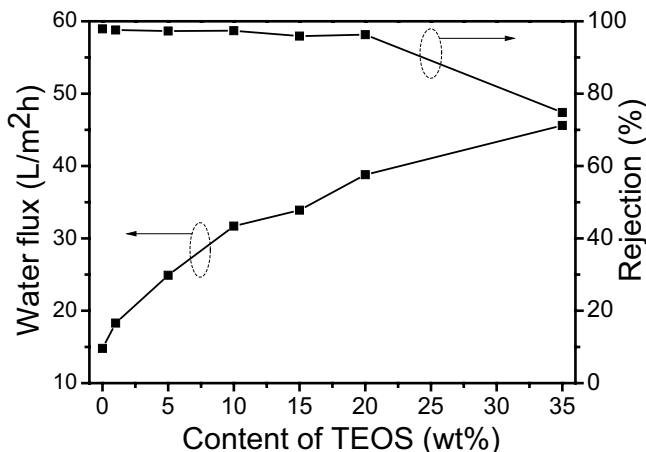


Fig. 7. Water flux and salt rejection of the nanocomposite membranes prepared with different TEOS contents.

co-solvent would lead to larger pore or deflection in the polyamide layer due to the further decrease in the degree of cross-linking of polyamide layer.

3.3. Effect of TEOS on MPD diffusivity/permeability

Researchers found that the MPD solubility and diffusivity in the organic phase influenced the polyamide thin-film structure and further affected the water permeability. The diffusivity of MPD was negatively proportional to the viscosity, while the solubility was positively proportional to the surface tension [35]. The surface tension and viscosity of hexane and TEOS were listed in Table 1.

It should be noted that the viscosity and surface tension of TEOS were both larger than that of *n*-hexane. Therefore, the addition of TEOS in *n*-hexane increased the viscosity and surface tension of mixed solvent. In order to verify the improved solubility, the diffusion trend of MPD from water phase to the organic phase was investigated. First, 5 mL of water phase (2 wt.%, 98 wt.% H₂O) was added to the test tube, and then 5 mL of *n*-hexane or mixed solvent (80 wt.% hexane, 20 wt.% TEOS) was slowly added and allowed to stand for 1, 2, 3, 4, and 5 min. Then the absorbance of the upper organic phase was measured by ultraviolet spectrophotometry. The results were shown in Fig. 8.

Fig. 8 shows that the absorbance increases with the increase in contact time. The absorbance could represent the MPD concentration, and the variation trend of MPD could

Table 1
Properties of solvents used to form RO membranes

	Hexane	TEOS
Surface tension (N m ⁻¹)	18	23
Viscosity (mPa s)	0.300	17.900

Data obtained for 25°C from “CRC Handbook of Chemistry and Physics,” David R. Lide, 84th Edition (2003–2004), CRC Press.

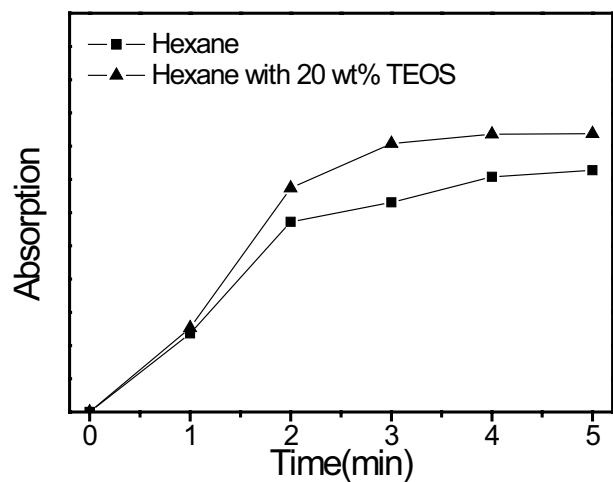


Fig. 8. The absorbance variation trend of MPD in organic layer at different time by UV spectrophotometry.

indicate the diffusion of MPD from the water phase to the organic phase. The absorbance of the organic solvent with the addition of TEOS was higher than that of the organic solvent without TEOS, indicating that the concentration of MPD was large in the organic solvent with the addition of TEOS. This meant higher concentration of MPD in the IP zone.

The addition of TEOS as co-solvent in the organic phase increased the viscosity and surface tension and then enhanced the solubility and reduced the diffusivity of MPD. The solubility and diffusivity of MPD affected the IP process and thus affected the degree of membrane cross-linking and membrane surface. Water permeability strongly correlated with MPD diffusivity and moderately correlated with MPD solubility, while salt permeability moderately correlated with MPD solubility and had little correlation with MPD diffusivity [35]. MPD solubility correlation reinforced the potential mechanistic connection between film structure (cross-linking) and effective membrane surface area [36–38]. Researchers found that the hydrophilicity, thickness, and the surface roughness of the membrane increased, while the membrane surface area and the degree of cross-linking decreased with the increase of the solubility of MPD in different organic solvents. In general, water flux was proportional to hydrophilicity and roughness but inversely proportional to membrane thickness and cross-linking [35].

3.4. Stability of membranes

The stability tests were conducted for 48 h at the operating pressure of 1.6 MPa with 2,000 ppm NaCl aqueous solution. As can be seen from Fig. 9, both the pure polyamide composite membrane and the nanocomposite membrane prepared with 20 wt.% TEOS had a drop of about 10% in water flux in the first 10 h of operation. It indicated that the modified membrane with TEOS was stable and similar to the pure polyamide membrane. Our previous study showed that the water flux decreased by near 20% after 10 h test for the modified polyamide membrane prepared with ethylformate as co-solvent [20]. The typical multilayered polyamide structure with large “valleys and ridges” formed through the IP assisted by co-solvent may be compacted

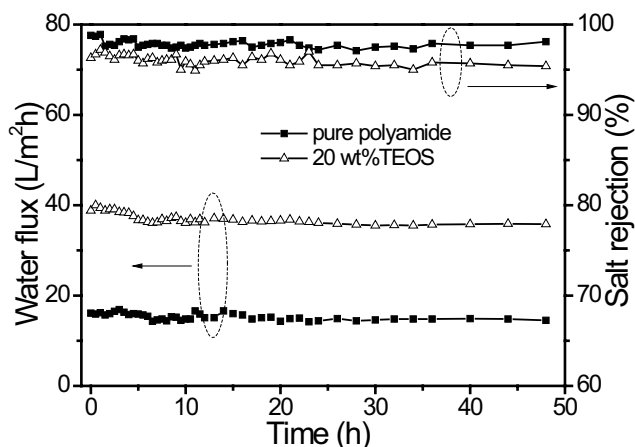


Fig. 9. Stability of the pure polyamide composite membrane and the nanocomposite membrane prepared with 20 wt.% TEOS.

during the filtration with higher pressure, leading to the decline of the water flux. During the formation process of polyamide layer and posttreatment, TEOS would undergo hydrolysis and condensation to form the solid silica particles and resided in the polyamide layer. It was different with the other co-solvents, such as alcohols, esters, and ketones, which did not change or react during the IP process, and heat treatment could be eliminated. Therefore, the TEOS-modified membrane had enhanced mechanical stability. This was the advantage of the TEOS as co-solvent, voiding the compaction of polyamide layer and the agglomeration of nanoparticles, which could combine the superiority of co-solvent and nanofiller method.

3.5. Mechanism of membrane formation assisted with TEOS

The schematic diagram of polyamide membranes was formed based on previous reports by Kong et al. [17], Kwak et al. [37], and Freger et al. [39]. With the MPD from the water phase to the organic phase diffusion, the deeper into the organic phase, MPD concentration was lower. Therefore, the network pore and aggregation pore became larger, resulting in lower cross-linking degree of the polyamide layer. As shown in Figs. 10(a) and (b), the diffusion distance of MPD with IP for 5 min was much longer than that of IP for 1 min, leading to larger peak valley structure and thickness of the polyamide layer. This was consistent with the surface morphology of the membrane shown in Figs. 4(a) and (b). The number of polyamide layers and the thickness increased with longer IP time, resulting in decrease in the water flux.

Due to slightly soluble in water, TEOS diffused to the water phase and consequently formed a relatively narrow miscible zone. As shown in Fig. 10(c), the reaction zone composed of organic reaction zone and miscible reaction zone. During the first period of the IP, MPD and TMC diffuse to the miscible phase. A loose widespread polyamide layer was quickly formed within this zone. Then, the MPD diffused through the initially formed loose polyamide layer and reacted with TMC at a slow rate in the organic reaction zone, leading to larger network pore and aggregate pore [16–19]. This was consistent with the surface morphology of the membrane shown in Figs. 4(b)–(g).

As shown in Fig. 10(c), since the molecular diameter of TEOS was relatively large, TEOS was encapsulated in the polyamide layer during the polymerization reaction. When the IP time was too short, the polyamide layer was defective, resulting in a low rejection and high water flux. Therefore, the IP time was prolonged to 5 min to ensure the thicker and perfect polyamide layer. As a result, encapsulated TEOS in the polyamide could transform to nanoparticles in situ by hydrolysis and condensation reaction.

Fig. 11 presents the SEM images of the cross section of the pure polyamide TFC membranes prepared with different IP times and the nanocomposite membranes prepared by adding TEOS with IP time for 5 min. It can be seen that the thicker polyamide layer could be obtained with IP for 5 min (Fig. 11(b)) than that of IP for 1 min (Fig. 11(a)). And the polyamide layer of the nanocomposite membranes prepared by adding TEOS is thicker than the pure polyamide TFC membrane. The results validate the above formation mechanism of the membranes.

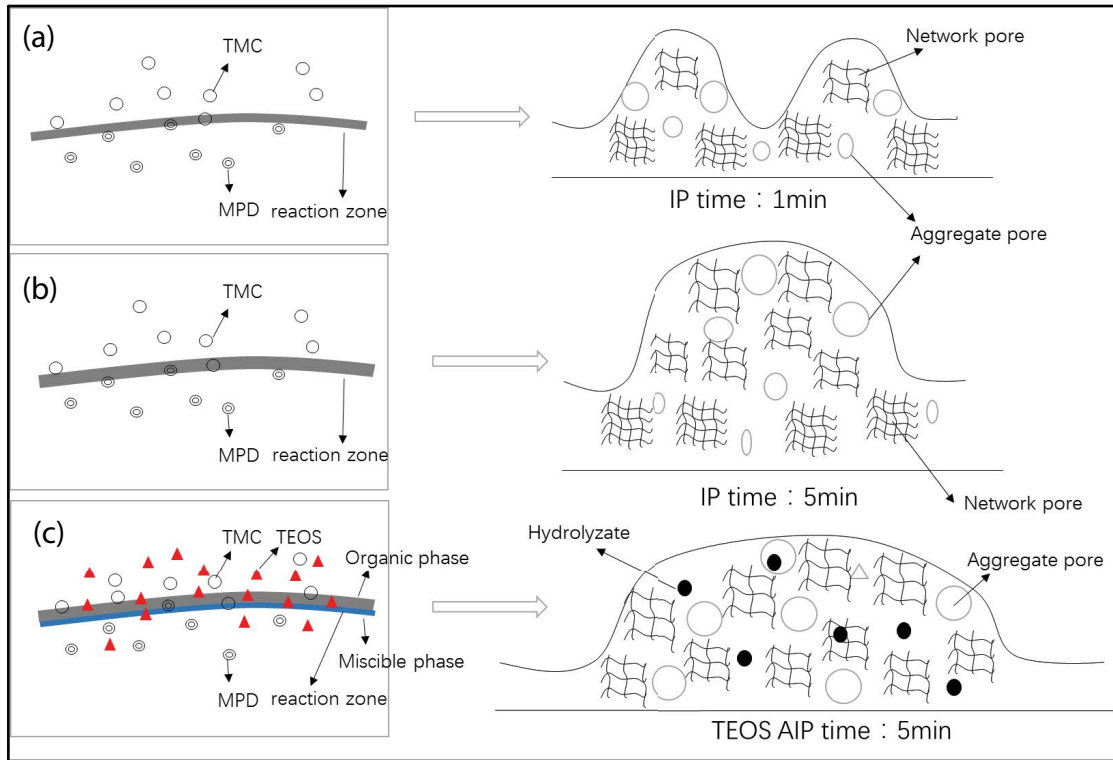


Fig. 10. Mechanism of the pure polyamide membranes prepared with different IP times: (a) 1 min and (b) 5 min, and the nanocomposite membranes prepared with TEOS with IP time for 5 min (c).

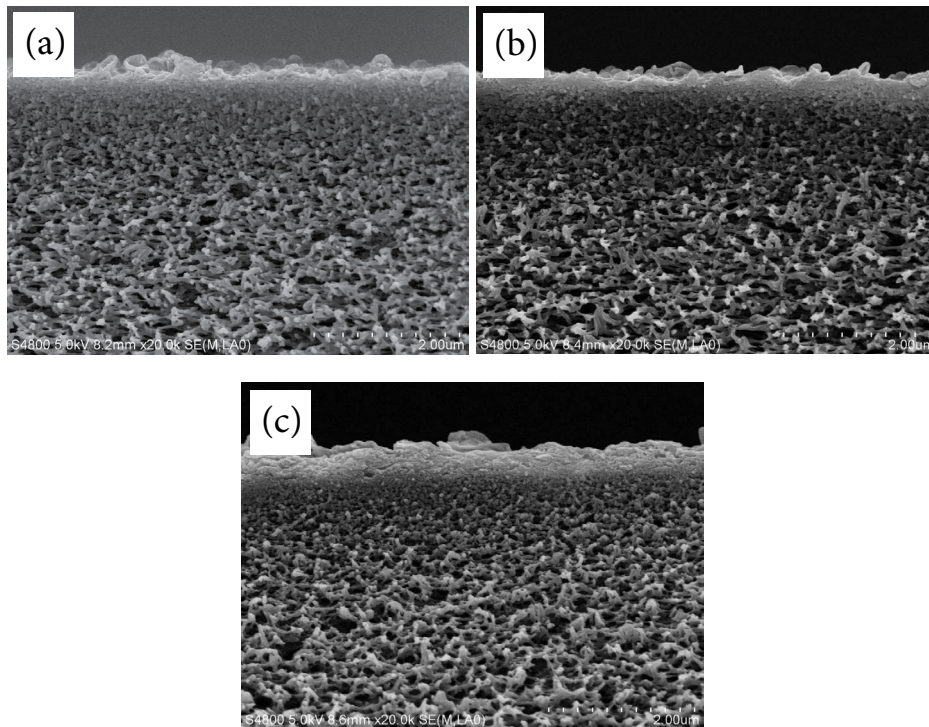


Fig. 11. SEM images of the cross section of pure polyamide thin-film composite membranes prepared with different IP times: (a) 1 min, (b) 5 min, and (c) the nanocomposite membranes prepared by adding TEOS with IP time for 5 min.

4. Conclusions

In summary, polyamide nanocomposite RO membrane with higher water flux and salt rejection was prepared with TEOS in the hexane solution. In the process of IP, TEOS not only acts as a co-solvent to improve the membrane structure to provide effective “nanopore” sizes but also hydrolyzes and condenses to produce hydrophilic silica in situ to improve membrane RO performance. Compared with the pure polyamide membrane, the nanocomposite membrane by TEOS-assisted IP showed high desalination performance. Such kill two birds with one stone strategy is very meaningful and worthy for further study.

Acknowledgements

The financial support from the National Natural Science Foundation of China (No. U1607124, 21276246) and the China Scholarship Council are gratefully acknowledged and Key Research Project of Shandong Province (No. 2017GHY215001).

References

- [1] T. Matsuura, Progress in membrane science and technology for seawater desalination—a review, *Desalination*, 134 (2001) 47–54.
- [2] B.V. der Bruggen, Desalination by distillation and by reverse osmosis—trends towards the future, *Membr. Technol.*, 2 (2003) 6–9.
- [3] D. Li, H. Wang, Recent developments in reverse osmosis desalination membranes, *J. Mater. Chem.*, 20 (2010) 4551–4566.
- [4] L.M. Fry, J.R. Mihelcic, D.W. Watkins, Water and nonwater-related challenges of achieving global sanitation coverage, *Environ. Sci. Technol.*, 42 (2008) 4298–4304.
- [5] C.S. Slater, R.C. Ahlert, C.G. Uchirin, Applications of reverse osmosis to complex industrial wastewater treatment, *Desalination*, 48 (1983) 171.
- [6] D. Bhattacharyya, M. Jevtitch, J.K. Ghosal, J. Kozminsky, Reverse osmosis membrane for treating coal-liquefaction wastewater, *Environ. Prog. Sustainable Energy*, 3 (1984) 95.
- [7] B.H. Jeong, E.M.V. Hoek, Y. Yan, A. Subramani, X. Huang, G. Hurwitz, A.K. Ghosh, A. Jawor, Interfacial polymerization of thin film nanocomposites: a new concept for reverse osmosis membranes, *J. Membr. Sci.*, 294 (2007) 1–7.
- [8] N. Niksefat, M. Jahanshahi, A. Rahimpour, The effect of SiO₂ nanoparticles on morphology and performance of thin film composite membranes for forward osmosis application, *Desalination*, 343 (2014) 140–146.
- [9] L. Liu, G. Zhu, Z. Liu, C. Gao, Effect of MCM-48 nanoparticles on the performance of thin film nanocomposite membranes for reverse osmosis application, *Desalination*, 394 (2016) 72–82.
- [10] H.J. Kim, M.Y. Lim, K.H. Jung, D.G. Kim, J.C. Lee, High-performance reverse osmosis nanocomposite membranes containing the mixture of carbon nanotubes and graphene oxides, *J. Mater. Chem. A*, 3 (2014) 6798–6809.
- [11] R. Cruz-Silva, S. Inukai, T. Araki, A. Morelos-Gomez, High performance and chlorine resistant carbon nanotube/aromatic polyamide reverse osmosis nanocomposite membrane, *MRS Adv.*, 1 (2016) 1469–1476.
- [12] E.S. Kim, B. Deng, Fabrication of polyamide thin-film nanocomposite (PA-TFN) membrane with hydrophilized ordered mesoporous carbon (H-OMC) for water purifications, *J. Membr. Sci.*, 375 (2011) 46–54.
- [13] H. Dong, L. Zhao, L. Zhang, H. Chen, C. Gao, High-flux reverse osmosis membranes incorporated with NaY zeolite nanoparticles for brackish water desalination, *J. Membr. Sci.*, 476 (2015) 373–383.
- [14] J. Duan, Y. Pan, F. Pacheco, E. Litwiller, Z. Lai, I. Pinnau, High-performance polyamide thin-film-nanocomposite reverse osmosis membranes containing hydrophobic zeoliticimidazole framework-8, *J. Membr. Sci.*, 476 (2015) 303–310.
- [15] M. Bao, G. Zhu, L. Wang, M. Wang, C. Gao, Preparation of monodispersed spherical mesoporous nanosilica–polyamide thin film composite reverse osmosis membranes via interfacial polymerization, *Desalination*, 309 (2013) 261–266.
- [16] C. Kong, M. Kanezashi, T. Yamamoto, T. Shintani, T. Tsuru, Controlled synthesis of high performance polyamide membrane with thin dense layer for water desalination, *J. Membr. Sci.*, 362 (2010) 76–80.
- [17] C. Kong, T. Shintani, T. Kamada, V. Freger, T. Tsuru, Co-solvent-mediated synthesis of thin polyamide membranes, *J. Membr. Sci.*, 384 (2011) 10–16.
- [18] T. Kamada, T. Ohara, T. Shintani, T. Tsuru, Optimizing the preparation of multi-layered polyamide membrane via the addition of a co-solvent, *J. Membr. Sci.*, 453 (2014) 489–497.
- [19] T. Kamada, T. Ohara, T. Shintani, T. Tsuru, Controlled surface morphology of polyamide membranes via the addition of co-solvent for improved permeate flux, *J. Membr. Sci.*, 467 (2014) 303–312.
- [20] Z. Liu, G. Zhu, Y. Wei, D. Zhang, J. Lei, H. Wang, C. Gao, Enhanced flux performance of polyamide composite membranes prepared via interfacial polymerization assisted with ethyl formate, *Water Sci. Technol.*, 76 (2017) 1884–1894.
- [21] X. Liu, Y. Peng, S. Ji, A new method to prepare organic–inorganic hybrid membranes, *Desalination*, 221 (2008) 376–382.
- [22] C.C. Yang, Y.J. Li, T.H. Liou, Preparation of novel poly (vinyl alcohol)/SiO₂ nanocomposite membranes by a sol–gel process and their application on alkaline DMFCs, *Desalination*, 276 (2011) 366–372.
- [23] A. Ananth, G. Arthanareeswaran, H. Wang, The influence of tetraethylorthosilicate and polyethyleneimine on the performance of polyethersulfone membranes, *Desalination*, 287 (2012) 61–70.
- [24] A. Ananth, G. Arthanareeswaran, Y.S. Mok, Effects of in situ and ex situ formations of silica nanoparticles on polyethersulfone membranes, *Polym. Bull.*, 71 (2014) 2851–2861.
- [25] H.P. Xu, Y.H. Yu, W.Z. Lang, X. Yan, Y.J. Guo, Hydrophilic modification of polyvinyl chloride hollow fiber membranes by silica with a weak in situ sol-gel method, *RSC Adv.*, 5 (2015) 13733–13742.
- [26] L. Wu, J. Sun, Z. Lv, Y. Chen, In-situ preparation of poly(ether imide)/aminofunctionalized silica mixed matrix membranes for application in enzyme separation, *Mater. Des.*, 92 (2016) 610–620.
- [27] M. Shafiq, A. Sabira, A. Islama, S.M. Khana, S.N. Hussain, M.T.Z.Z. Butt, T. Jamila, Development and performance characteristics of silane crosslinked poly (vinyl alcohol)/chitosan membranes for reverse osmosis, *J. Ind. Eng. Chem.*, 48 (2017) 99–107.
- [28] G. Gong, J. Wang, H. Nagasawa, M. Kanezashi, T. Yoshioka, T. Tsuru, Fabrication of a layered hybrid membrane using an organosilica separation layer on a porous polysulfone support, and the application to vapor permeation, *J. Membr. Sci.*, 464 (2014) 140–148.
- [29] G. Gong, J. Wang, H. Nagasawa, M. Kanezashi, T. Yoshioka, T. Tsuru, Synthesis and characterization of a layered-hybrid membrane consisting of an organosilica separation layer on a polymeric nanofiltration membrane, *J. Membr. Sci.*, 472 (2014) 19–28.
- [30] C.L. Kong, A. Koushima, T. Kamada, T. Shintani, M. Kanezashi, T. Yoshioka, T. Tsuru, Enhanced performance of inorganic-polyamide nanocomposite membranes prepared by metal-alkoxide-assisted interfacial polymerization, *J. Membr. Sci.*, 366 (2011) 382–388.
- [31] W. Ding, Y. Li, M. Bao, J. Zhang, C. Zhang, J. Lu, Highly permeable and stable forward osmosis (FO) membrane based on the incorporation of Al₂O₃ nanoparticles into both substrate and polyamide active layer, *RSC Adv.*, 7 (2017) 40311–40320.
- [32] S.Y. Kwak, S.G. Jung, S.H. Kim, Structure–motion–performance relationship of flux-enhanced reverse osmosis (RO) membranes composed of aromatic polyamide thin films, *Environ. Sci. Technol.*, 35 (2001) 4334–4340.

- [33] A. Peyki, A. Rahimpour, M. Jahanshahi, Preparation and characterization of thin film composite reverse osmosis membranes incorporated with hydrophilic SiO₂ nanoparticles, *Desalination*, 368 (2015) 152–158.
- [34] W. Ding, H. Zhuo, M. Bao, Y. Li, J. Lu, Fabrication of organic-inorganic nanofiltration membrane using ordered stacking SiO₂ thin film as rejection layer assisted with layer-by-layer method, *Chem. Eng. J.*, 330 (2017) 337–344.
- [35] K.A. Ghosh, B.H. Jeong, X. Huang, E.M.V. Hoek, Impacts of reaction and curing conditions on polyamide composite reverse osmosis membrane properties, *J. Membr. Sci.*, 311 (2008) 34–45.
- [36] C.K. Kim, J.H. Kim, I.J. Roh, J.J. Kim, The changes of membrane performance with polyamide molecular structure in the reverse osmosis process, *J. Membr. Sci.*, 165 (2000) 189–199.
- [37] S.H. Kim, S.Y. Kwak, T. Suzuki, Positron annihilation spectroscopic evidence to demonstrate the flux-enhancement mechanism in morphology controlled thin-film-composite (TFC) membrane, *Environ. Sci. Technol.*, 39 (2005) 1764–1770.
- [38] S.Y. Kwak, D.W. Ihm, Use of atomic force microscopy and solid-state NMR spectroscopy to characterize structure-property-performance correlation in high-flux reverse osmosis (RO) membranes, *J. Membr. Sci.*, 158 (1999) 143–153.
- [39] V. Freger, Kinetics of film formation by interfacial polycondensation, *Langmuir*, 21 (2005) 1884–1894.